Negative Reversibly Switchable Fluorescent Proteins

Subjects: Biophysics

Contributor: Chong Fang, Longteng Tang

The advancement of super-resolution imaging (SRI) relies on fluorescent proteins with novel photochromic properties. Using light, the reversibly switchable fluorescent proteins (RSFPs) can be converted between bright and dark states for many photocycles and their emergence has inspired the invention of advanced SRI techniques. The general photoswitching mechanism involves the chromophore *cis-trans* isomerization and proton transfer for negative and positive RSFPs and hydration–dehydration for decoupled RSFPs. However, a detailed understanding of these processes on ultrafast timescales (femtosecond to millisecond) is lacking, which fundamentally hinders the further development of RSFPs. For a negative RSFP such as Dronpa, the light used to induce fluorescence can often switch the protein from the on to off state; whereas for a positive RSFP like Padron, the same light can turn more proteins on. In contrast, the decoupled RSFPs can use separate light with different wavelengths for fluorescence excitation and photoswitching.

Keywords: photoswitchable fluorescent proteins ; ultrafast techniques ; cis-trans isomerization ; proton transfer ; molecular reaction dynamics ; excited state processes ; photochemistry

1. Introduction

Fluorescent protein (FP)-based microscopy and nanoscopy have revolutionized the bioimaging and life sciences for the past three decades [1][2][3][4]. On the imaging front, the commonly encountered low spatial resolution (~200 nm) of conventional fluorescence microscopy limits its applications in the detection of subcellular structures. Because of the development of various FP-based optical highlighters, super-resolution imaging has emerged to overcome the diffraction barrier, culminating in the 2014 Nobel Prize in Chemistry [5][6][7][8][9][10]. Among three types of optical highlighters, the photoswitchable fluorescent proteins, also known as reversibly switchable fluorescent proteins (RSFPs), have the advantage of switching back and forth between bright and dark states for multiple photocycles [11][12]. In contrast, the fluorescence of photoconvertible and photoactivatable FPs can only be transformed to a different color or bright state irreversibly [13][14].

Since the discovery of the first RSFP called asFP595 (tetrameric) in 2000 [15], many RSFPs with monomeric states, long emission wavelengths, high photostability, fast maturation, and high photoswitching quantum yield (PQY) have been developed [16][17][18][19]. In general, they can be classified into three categories: negative, positive, and decoupled types [20]. For most RSFPs, the photoswitching light and the fluorescence-excitation light are coupled. For a negative RSFP such as Dronpa [21], the light used to induce fluorescence can often switch the protein from the on to off state; whereas for a positive RSFP like Padron [22], the same light can turn more proteins on. In contrast, the decoupled RSFPs can use separate light with different wavelengths for fluorescence excitation and photoswitching [11]. Notably, almost all known RSFPs are either negative or positive types while the decoupled RSFPs have been rarely discovered. To date, Dreiklang and SPOON represent the only two reported decoupled RSFPs [23][24], and none has been reported to be engineered from the positive or negative RSFPs, substantiating their system-dependent nature (e.g., no cross over between the negative/positive and decoupled RSFP categories).

RSFPs typically adopt a soda-can structure similar to wild-type green fluorescent protein (wtGFP) with the chromophore (CRO) embedded at the β-barrel center (**Figure 1**a), which can be modeled as *p*-hydroxybenzylidene-2,3-dimethylimidazolinone (*p*-HBDI). To uncover the structure of RSFPs in bright and dark states, X-ray crystallography, steady-state electronic spectroscopy, and molecular dynamics (MD) simulations have been widely implemented. The current consensus about photoswitching pathways is that they involve the *cis-trans* isomerization and protonation state change of the chromophore for most RSFPs (Figure 1b), except the decoupled ones. The researchers note that the *cis-trans* isomerization has been extensively studied in the gas phase for molecules like azobenzene and retinal, especially on the femtosecond (fs) to picosecond (ps) timescales, but the retrieved mechanistic information cannot be simply transferred to the condensed phases (e.g., a protein matrix) due to the local environment change and the resultant difference in molecular Hamiltonian and density matrix. During the chromophore transformation, the surrounding protein

residues also need to relocate or reorient to accommodate the chromophore. However, only knowing the protein structures at the starting and ending states of the photoswitching events is not sufficient. Key information regarding the detailed switching routes after photoexcitation is still lacking, which lies at the molecular level to fundamentally determine the switching rate and efficiency.

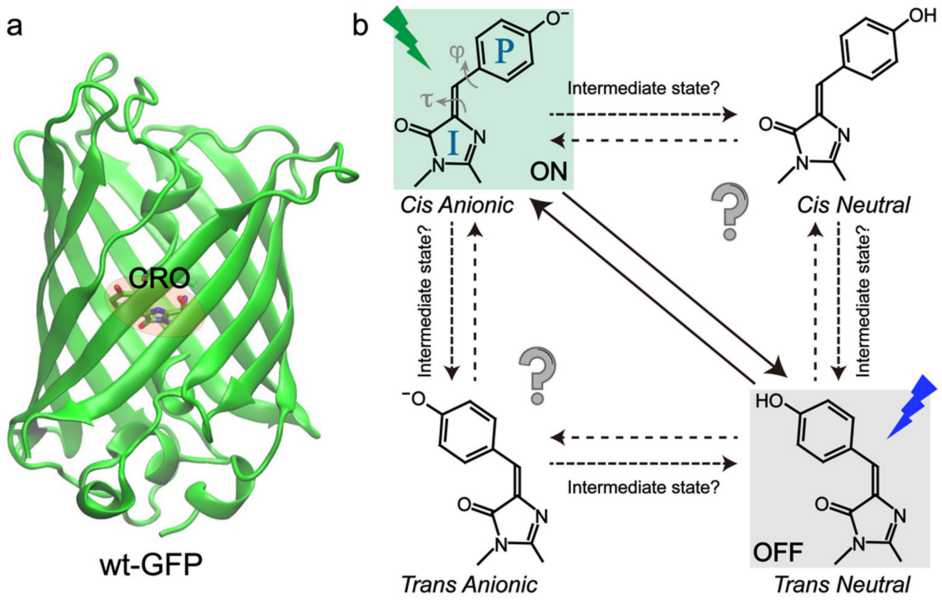

Figure 1. Schematic of the overall structure and photoswitching mechanisms of RSFPs. (**a**) Crystal structure of the wild-type green fluorescent protein (wtGFP) (PDB ID: 1EMA) [25]. (**b**) The photoinduced structural and protonation state changes of the chromophore (P- and I-rings denoted in the "ON" state) during reversible switching. Possible transitions and associated intermediate states are indicated by a network of solid and dashed arrows.

2. Negative RSFPs

2.1. Dronpa and Dronpa-2

Dronpa is the first monomeric negative RSFP engineered from coral *Pectiniidae* by Miyawaki et al. in 2004 [21]. It adopts an autocatalytically formed Cys62-Tyr63-Gly64 (CYG) chromophore [26]. In the resting state at pH 7.4, the majority of Dronpa is in a bright/on state with a dominant absorption peak at 503 nm, corresponding to the *cis*-anionic chromophore [27][28][29]. A minor absorption peak at 390 nm is due to the neutral chromophore. Irradiation at 490 nm generates strong fluorescence centered at 518 nm with a high fluorescence quantum yield (FQY) of 0.85. The 490 nm light can also transform Dronpa from the native on state to a dark/off state, adopting the *trans*-neutral chromophore, with a measured photoswitching quantum yield (PQY) of 3.2×10^{-4} [26][30]. A 400 nm light quickly converts the protein to its on state with an off-to-on PQY of 0.37 [21]. The development of Dronpa made it possible to track fast protein dynamics in living cells. To improve the PQY of Dronpa, rsFastLime was developed via a single V157G mutation to reduce steric opposition to a *trans* chromophore [28][31]. It displays a much faster on-to-off switching rate and PQY (3.5×10^{-3}) and only a small sacrifice of the FQY (0.77) versus Dronpa, making it a promising tool for bioimaging applications [28][32]. Dronpa-2 and Dronpa-3 were then developed with the single (M159T) and double (V157I and M159A) mutations with even higher on-to-off PQY values of 4.7×10^{-2} and 5.3×10^{-3}, respectively [33]. They were also able to quickly return to their bright state under dark adaptation. Notably, the on-to-off and off-to-on switching speeds of Dronpa-2 are more than 1100- and 2-fold faster than the rates of Dronpa in whole-cell imaging measurements [28]. However, these mutations come with a significant sacrifice of the FQYs (0.33 [33] or 0.23 [28] for Dronpa-2 and 0.28 [33] for Dronpa-3), which is understandable due to the ultrafast competition nature between the chromophore radiative and nonradiative pathways after photoexcitation [34]. The low FQY/brightness of Dronpa-2 limits its application in cellular imaging but its high PQY and switching rates render it suitable for ultrafast studies.

The first picosecond (ps) investigation of Dronpa in buffer solutions was performed by Habuchi et al. in 2005, using time-resolved fluorescence with single photon counting technique [35]. They discovered that Dronpa in the on state has a long lifetime of 3.6 nanoseconds (ns) following photoexcitation at 488 nm, in accord with its high FQY (0.85). The low-pH-induced protonated form can quickly return to the ground state with an average time constant of ~14 ps after 390 nm excitation in aqueous buffer at pH 7.4. Unlike the photoinduced protonated form, this low-pH-induced chromophore population lacks the photoconversion capability. On the single-molecule level, bright Dronpa can be switched to a dark

state which has a 65 ms lifetime to return to the on state. This research pinpointed characteristic photoswitching timescales and laid the foundation for future ultrafast investigations. Given that the retrieved time constants span from ps to ms, ultrafast techniques with fs resolution and ms detection window are needed for an in-depth mechanistic investigation, especially implementing the experimental toolsets that are structurally sensitive (e.g., vibrational spectroscopies and crystallography).

Two years later, Fron et al. implemented fs transient absorption (fs-TA) with a 395 nm photoexcitation pulse to target the off-to-on photoswitching process of Dronpa [36]. By contrasting the fs-TA spectral dynamics between the low-pH-induced and photoinduced protonated forms around the 420 nm probe region (following 395 nm excitation in aqueous buffer at pH 8.0), they discovered that the photoconverted protonated form in the off state exhibits a unique 4 ps process, which was attributed to excited-state proton transfer (ESPT) as supported by the observed deuterium (D)/hydrogen (H) kinetic isotope effect of ~2. However, this particular assignment was based on the dynamics of a rather noisy TA band in a highly overlapped region between the excited-state absorption (ESA) band of the deprotonated chromophore around 420 nm and the stimulated emission (SE) band of the protonated chromophore species around 450 nm [37], so its probe-dependent fits were likely convoluted and complex to interpret. In addition, the 4 ps component was characterized as a decay process; if the 420 nm signal indeed originated from the ESA band of a deprotonated chromophore, a prominent ESPT step would lead to a rise component at this wavelength on the aforementioned timescale. The ultrafast ESPT argument was later challenged by several ultrafast studies (see below). Moreover, this research [36] offered little information about the protein structural evolution.

In 2013, the off-to-on photoactivation of Dronpa was revisited by Warren et al. with a fs vibrational technique, time-resolved infrared (TRIR) spectroscopy, for the first time [38]. They focused on the high-frequency vibrational region of the photoswitched Dronpa after 400 nm excitation in aqueous buffer solution at pH or pD 7.8. Global analysis of the TRIR spectra with a sequential model revealed a short-lived species with a 9 ps lifetime and a long-lived species (**Figure 2**). Because the *cis*-anionic chromophore displays a characteristic C=C stretching mode at 1655 cm^{-1} and phenol-1 mode at 1623 cm^{-1} based on the static FTIR difference (on minus off) spectra, which are both absent in the spectra of the long-lived species (**Figure 2**a), the authors concluded that proton transfer is a ground state process while the 9 ps transition time was attributed to the decay of the *trans*-neutral chromophore (likely involving the ultrafast *trans-cis* isomerization to result in a *cis*-neutral chromophore) in the excited state. They also monitored the $CN_3H_5^+$ stretching band of Arg66 (an adjacent protein residue) and the C=O band of the chromophore (HBDI embedded in the protein pocket, **Figure 1**a) starting from the on state after photoexcitation and showed that hydrogen (H)-bond weakening between the chromophore and local residues is highly related to the much less efficient on-to-off switch (PQY ≈ 3×10^{-4}) than the off-to-on switch (PQY ≈ 0.3). This work represents an important contribution because it demonstrated that ultrafast vibrational spectroscopy, which is intrinsically sensitive to molecular structural changes, can track the chromophore isomerization processes of RSFPs in real time. Moreover, the capability of TRIR to probe the vibrational bands of surrounding residues demonstrates the importance of protein residues in the chromophore vicinity in determining the photoswitching rate and efficiency of the overall protein. However, the spectral and temporal detection window (~140 cm^{-1} and up to 100 ps, respectively) in this research were rather narrow, which limits efforts in building a more comprehensive model based on the spectral data.

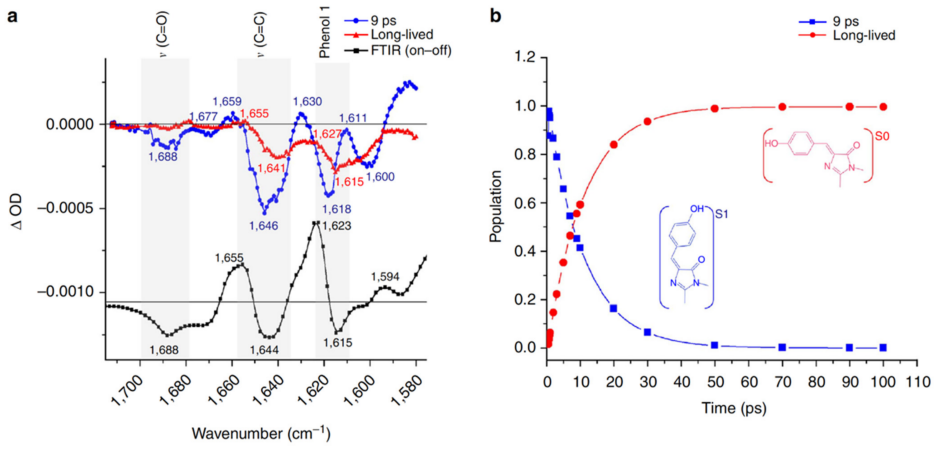

Figure 2. Time-resolved infrared (IR) spectroscopy reveals characteristic species during the off-to-on photoswitching of Dronpa after 400 nm excitation. (**a**) Time-resolved difference spectra (pump-on minus pump-off) retrieved from global analysis with a sequential model (blue→red) and the FTIR difference spectra between the on and off states in D_2O (black). (**b**) Global fitting results of the short-lived (blue) and long-lived (red) species with a dominant 9 ps component due

to the decay of the singlet excited state of the *trans*-neutral chromophore (blue structure shown in the inset). Reprinted with permission from Ref. [38]. Copyright 2013 The Authors.

Later in the same year, Lukacs et al. implemented TRIR and investigated a Dronpa mutant, Dronpa-2, because of its high PQYs between the on and off states [39]. They were able to cover a much broader window over 300 cm^{-1} in transient IR spectra and up to a few hundreds of ps after 400 nm photoexcitation, enabling the tracking of more protein modes on the sub-ns timescale. In this research, they discovered that the nearby conserved E144 residue in Dronpa-2 (corresponding to E222 in wtGFP [25][40]), which is H-bonded to the phenolic end of the chromophore through an intervening water molecule and is the potential proton acceptor for the ESPT reaction [29][30][41], does not exhibit a rise of the carbonyl mode at 1710 cm^{-1} and decay of the carboxylate mode at 1560 cm^{-1}, both of which are TRIR signatures for the ESPT process in wtGFP. This finding agreed with Warren et al.'s result that the proton transfer is a ground-state thermal process [38]. However, since Lukacs et al. did not observe a blueshift of the C=O mode at ~1690 cm^{-1} that was considered as a signature for *trans*-to-*cis* isomerization, they concluded that the chromophore torsion does not occur on the ps timescale, contradictory to Warren et al. [38]. Instead, they speculated that on the sub-ns timescale (starting from the ps radiationless relaxation), the H-bonding network reorganization in the chromophore vicinity constitutes the dominant process, leading to the formation of a metastable ground state, and the subsequent isomerization would occur on much longer timescales beyond the ns regime. Their explanation of the sub-ns H-bonding network rearrangement between the chromophore and local residues sheds some light on the small kinetic isotope effect (~2) that was observed on the ~4 ps timescale [36], because restructuring of a rather flexible H-bonding network does not need to involve highly directional proton motions from the chromophore and hence reduce the proton transfer rate difference upon deuteration [40][42]. Nevertheless, the exact nature of that metastable ground state remains unclear, which requires further investigations with high-level quantum calculations and spectroscopic techniques with even longer detection time windows (e.g., ms timescale).

Overall, regarding the off-to-on photoactivation mechanisms of Dronpa and Dronpa-2, multiple ultrafast techniques including time-resolved fluorescence, fs/ns-TA and TRIR, which cover various spectral and temporal ranges, have been implemented. The current consensus about this process is that the chromophore *trans-cis* isomerization precedes GSPT. However, whether or not the isomerization occurs in the excited or ground state remains debated while the retrieved time constants and associated interpretations are still inconsistent across different techniques. In addition, even the reported PQYs and FQYs of Dronpa and Dronpa-2 have notable variations in literature [21][22][43][44][45]. Furthermore, all studies could not identify the exact chromophore twisting structures or coordinates in the excited or ground state. Therefore, novel ultrafast techniques, such as femtosecond stimulated Raman spectroscopy (FSRS) [34][40][46][47] and the time-resolved serial femtosecond crystallography [48], as well as high-level quantum calculations and molecular dynamics simulations [49] [50] are needed to further elucidate the detailed switching pathways inside RSFPs.

2.2. RsEGFP2

RsEGFP2 is an engineered descendent of the well-known wtGFP, which was discovered from the Pacific Northwest jellyfish *Aequorea victoria* (Hydrozoa) in 1962 [51] and adopts a Ser65-Tyr66-Gly67 (SYG) chromophore [2][52]. To improve the brightness of wtGFP, two point mutations (S65T and F64L) were carried out to yield an enhanced GFP (EGFP) in 1996 with 35-fold more fluorescence intensity and an FQY of ~0.60 [53]. In 2011, Grotjohann et al. developed an EGFP-based monomeric RSFP named reversibly switchable EGFP (rsEGFP) by introducing additional mutations (Q69L, V150A, V163S, S205N, and A206K) to EGFP via site-directed and error-prone mutagenesis [8]. RsEGFP was able to undergo ~1100 cycles of photoswitching before its fluorescence intensity decays by 50% and the switching rate is more than 10-fold faster than Dronpa (see Section 2.1 above). However, rsEGFP was still rather slow when implemented in the subdiffraction-resolution RESOLFT microscopy that employs the reversible saturable optical fluorescence transitions between two (on and off) states in a spatially targeted manner. In 2012, Grotjohann et al. continued to develop rsEGFP2 with only four mutations (T65A, Q69L, V163S, and A206K) based on EGFP [54]. RsEGFP2 adopts an Ala65-Tyr66-Gly67 (AYG) chromophore and was able to record images in RESOLFT 25–250 times faster than rsEGFP. At pH 7.5, rsEGFP2 rests in its bright state with an excitation maximum at 478 nm and a fluorescence peak around 503 nm. A 480 nm light can induce fluorescence from rsEGFP2 with FQY ≈ 0.30 but can also bleach it (yet the fluorescence was halved not before ~2100 cycles of photoswitching [54]), and 400 or 405 nm irradiation activates it again. The on-to-off and off-to-on PQYs of rsEGFP2 are 1.65×10^{-2} and 0.33, respectively [55], later reported as 0.04 and 0.40 [56] or 0.01 and 0.18 [57]. Based on its crystal structure in the on and off states with specific H-bonding patterns, the photoswitching mainly involves the *cis-trans* isomerization and proton transfer, similar to other negative RSFPs [11]. Notably, since both one-bond flip and hula twist can lead to the formation of a *trans*-chromophore, a recent study by Chang et al. revealed that for rsEGFP2, the protein packing in the crystal lattice is a determining factor for the photoswitching pathways: a loose and tight packing configuration leads to the one-bond flip and hula twist, respectively [58].

In 2018, Coquelle et al. performed the first ultrafast study on rsEGFP2 with fs-TA and time-resolved serial femtosecond crystallography (TR-SFX), focusing on its early time (sub-ns) structural change [56]. Guided by the fs-TA spectra of rsEGFP2 in aqueous solution (pH/pD 8) which exhibit a strong signal at ~1 ps and a significant decay at 3 ps, they collected the TR-SFX data at the two delay time points after 400 nm photoexcitation. They resolved two conformers (model P (planar) and model T (twisted)) at 1 ps (**Figure 3**a), but only model T and the *cis* structure were clearly observed at 3 ps (**Figure 3**b). This key result indicated that the *trans-cis* isomerization has already occurred by 3 ps following electronic excitation. The structure of Model P closely resembles the off state (**Figure 3**a) while the geometry of model T is in between the *cis* and *trans* geometries (**Figure 3**b). The existence of two conformers was supported by their excited-state quantum mechanics/molecular mechanics (QM/MM) and classical MD simulations. Because twisting of the *trans*-chromophore to form model T, which is the precursor of the *cis*-form, involves both dihedral angles, they attributed the photoactivation of rsEGFP2 to a hula-twist mechanism. In the resolved crystal structure of rsEGFP2 at 3 ps (**Figure 3**b), V151 sterically hinders further motions in model T at the phenol side, so the authors performed a targeted mutation (V151A) to reduce the hindrance: the off-to-on PQY of the new rsEGFP2 mutant almost doubles when compared to the parent protein based on their PQY measurements. However, they later discovered that the measurement was incorrect and there is no significant difference between the PQYs of rsEGFP2 and rsEGFP2-V151A [59]. This result showcases the complexities in point mutations which may also induce additional changes to the chromophore's surrounding residues that can lead to an outcome deviated from expectations. The study by Coquelle et al. offered a good example of utilizing ultrafast spectroscopic techniques, in combination with quantum and classical calculations to retrieve the underlying molecular mechanisms. However, unresolved questions linger from this research [56]. For example, the fs-TA spectra reveal three excited states: a Franck–Condon state with a 90 fs decay and two additional intermediate states with 0.9 and 3.7 ps decay time constants. The nearly planar Model P was attributed to one state whereas the twisted Model T was attributed to neither state because its calculated transition dipole moment is close to zero. The exact nature of the other state was unclear, while the SE band dynamics near the deprotonated chromophore fluorescence peak (~503 nm) could be further analyzed. Moreover, the research offered no information about the photoactivation process of rsEGFP2 on longer timescales (e.g., ns to ms).

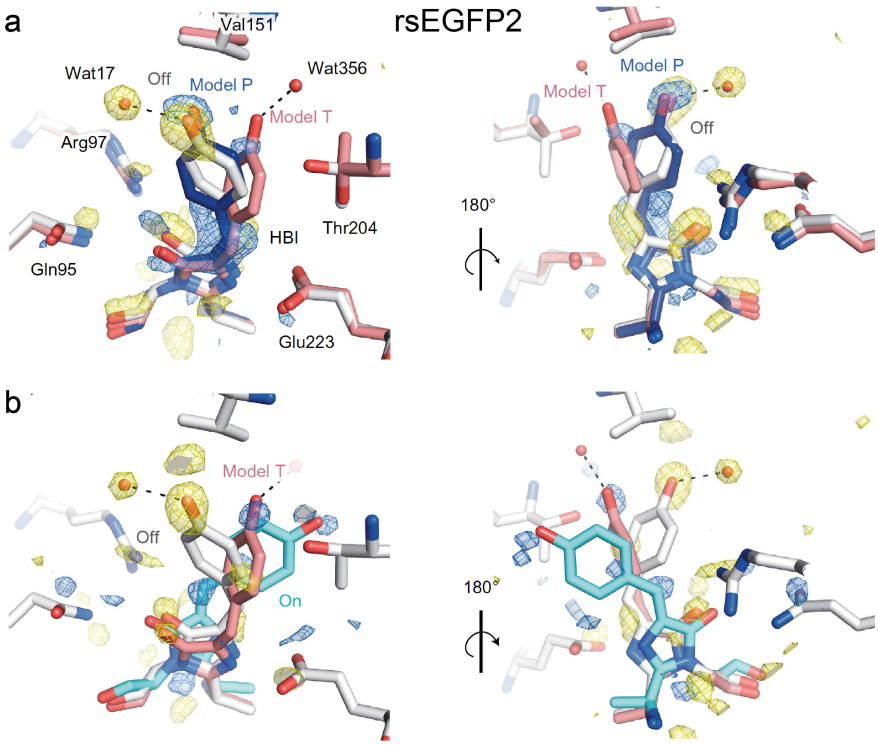

Figure 3. Local structure of rsEGFP2 in the first singlet electronic excited state modeled from difference Fourier electron-density maps of SFX data. (**a**) Comparison of Model P (blue), Model T (pink), and the off state (gray) against SFX map at 1 ps after photoexcitation (PDB ID: 5O8B) [56]. (**b**) Comparison of Model T (red) with the off (gray) and on (cyan; PDB ID: 5O89) states against SFX map at 3 ps after photoexcitation. Note that in model T, the twisted chromophore features perpendicular phenol and imidazolinone rings. Key surrounding residues are shown with the H-bond denoted by dashed lines. Reprinted with permission from Ref. [56]. Copyright 2017 Macmillan Publishers Limited, part of Springer Nature.

Subsequently in 2020, Woodhouse et al. studied rsEGFP2 again with TA and TR-SFX but focused on the longer timescale beyond ps [60]. They collected the TR-SFX data of rsEGFP2 at 10 ns and observed that the chromophore is already in the *cis* geometry on this timescale, the same as the "target" on state but prior to chromophore deprotonation on the µs-to-ms timescale (see above). However, the side chain of the adjacent residue His149 is still at an off-like position (**Figure 4**);

note these SFX data were modeled with ~10% remaining on-state population and other inhomogeneous conformational species (including a key residue His149 within H-bonding distance of the chromophore phenolic end). Global analysis of the fs-TA data of rsEGFP2 in its off state upon photoexcitation in aqueous buffer solution (pH 8) from 40 ps to 2 ns retrieved a single lifetime of 87 ps, which was attributed to the reorganization of the protein pocket to accommodate the *cis*-chromophore. Global analysis of the ns-TA data from 100 ns to 10 ms yielded three time constants of 5.57, 36.1, and 825 μs, with the latter two components exhibiting H/D kinetic isotope effect of ~2.5 that corresponds to GSPT steps, reminiscent of similar processes in Dronpa-2 [44][61]. The 5.57 μs component could arise from the reorganization of His149 or the other surrounding residues. Structural information about the nature of the 87 ps and 5.57 μs components was lacking in this research.

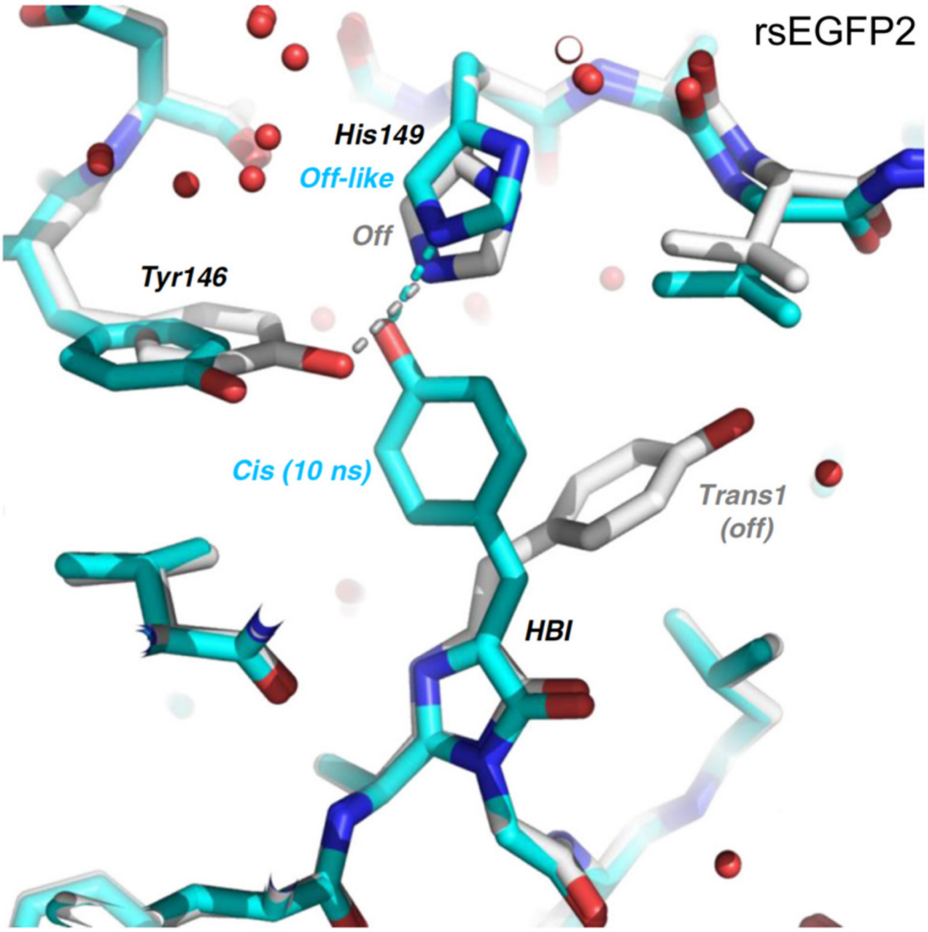

Figure 4. The 10 ns structure of rsEGFP2 during photoactivation. The *cis*-chromophore in the 10 ns intermediate (cyan; PDB ID: 6T3A) is overlaid with the *trans*-chromophore in the off state (gray, 65% occupancy major conformer), accompanied by a notable H-bonding partner change of His149 in off state (to Tyr146) versus 10 ns intermediate (to chromophore), denoted by the color-coded dashed lines. Reprinted with permission from Ref. [60]. Copyright 2020 The Authors.

To reveal the unresolved intermediate states on the ps and μs timescale from the previous two studies [56][60], Uriarte et al. recently implemented fs-to-ms time-resolved multiple-probe infrared spectroscopy (TRMPS-IR) with the Savitzky–Golay derivative filter to study rsEGFP2 in solution [57]. Global analysis of the IR spectra from 1 ps to 2 ns revealed three DADS with time constants of 0.7, 5.5, and 117 ps, similar to the 0.9, 3.7, and 87 ps from earlier reports [56][60]. The 0.7 ps DADS is characterized by a decay of the 1681 cm^{-1} C=O stretch band and rise of a positive 1686 cm^{-1} band. This characteristic blueshift from 1681 to 1686 cm^{-1} is a signature of *trans*-to-*cis* isomerization that indicates the formation of a *cis*-photoproduct precursor on this sub-ps timescale (i.e., a highly efficient ring twist). The result is consistent with the observation of the Model T chromophore at 1 ps from the TR-SFX experiment [56]. During the 5.5 ps transition time, only the recovery of vibrational bands from the *trans*-neutral chromophore was observed; thus, it was attributed to the relaxation of a hot planar *trans*-chromophore back to the original off state. On the 117 ps timescale, a further blueshift of the 1686 cm^{-1} mode to 1691 cm^{-1} was detected, suggesting that the chromophore continues to twist to its final *cis*-neutral state, similar to the 10 ns structure (**Figure 4**) observed in TR-SFX [60]. On longer timescales from 1 ns to 900 μs, four DADS were retrieved, including a new 42 ns component that had not been resolved from previous TA data. This component leads to a significant change in the 1651 cm^{-1} amide band from protein residues close to the chromophore, likely the His194 side chain (see **Figure 4**). No significant change in the TRIR spectra occurs on the 2.2 μs timescale,

likely associated with residues distant from the chromophore, such as the β-barrel relaxation (**Figure 1**a). Similar to the 10 ns TR-SFX reesarch [60], Uriarte et al. also observed two time constants of ~67 μs and 2 ms which were attributed to GSPT due to the appearance of a phenolate vibrational band at 1491 cm^{-1} [57]. Overall, by following the detailed dynamic patterns of carefully filtered vibrational marker bands, this most recent research supported the major conclusions from the TR-SFX investigations [56][60] and also discussed the previously hidden 42 ns process. Their results can be further verified by high-level excited/ground state quantum calculations and MD simulations (e.g., for accurate IR mode assignments) as well as targeted mutations of the protein.

Although the first ultrafast research of rsEGFP2 (hydrozoan origin) appeared more than 10 years later than Dronpa (anthozoan origin), a clearer photoactivation picture has been drawn for rsEGFP2. The timescale and sequence of isomerization and proton transfer are relatively consistent across various time-resolved electronic (TA) and vibrational (IR) spectroscopies. More importantly, the excited-state intermediate structures that govern the photoisomerization efficiency and rate have been solved, as well as the ground-state structure during further chromophore and protein relaxation. The experimental results have been correlated with theoretical calculations. However, only three crystal structures of rsEGFP2 at 1, 3 ps [56] and 10 ns [60] were solved, which limits painting a more comprehensive photoinduced reaction portrait. Investigations on the finer chromophore and surrounding pocket structures between ps and ns as well as beyond the μs timescale, also for RSFPs in physiological environments such as aqueous buffer solution under irradiation, can fill the missing links during off-to-on switching and offer additional important insights into the photoactivation pathways of RSFPs in living systems.

2.3. IrisFP

IrisFP was engineered from EosFP, which is a stony-coral-derived (anthozoan) green-to-red photoconvertible tetrameric fluorescent protein with a His62-Tyr63-Gly64 (HYG) chromophore [62], through a single-site F173S mutation [63]. Comparing to Dronpa and rsEGFP2, IrisFP inherited the photoconversion capability from its ancestor and it can also photoswitch reversibly within its green and red forms. The unique multi-photochromic behavior of IrisFP makes it a promising tool for advanced bioimaging applications. In aqueous buffer solution at pH 9, IrisFP exists in its green form with a major absorption band at ~488 nm and a minor band around ~390 nm. Excitation at 488 nm yields strong fluorescence at 516 nm with an FQY of 0.43. The 488 nm light can also convert the protein to an off state that absorbs at ~390 nm, with an on-to-off PQY of 0.014. A 405 nm light has the dual function to efficiently turn the protein back on (PQY ≈ 0.5) and convert the protein to red form (photoconversion QY ≈ 0.0018). The red species absorbs strongly at ~551 nm and emits at 580 nm with an FQY of 0.47, comparable to the green form. The red form can also be switched between its on and off states by the 532 and 440 nm light separately, with a much-reduced PQY (on-to-off ~0.0020, off-to-on ~0.047) when compared to the green species. Note that the off-to-on PQY is consistently much larger than the on-to-off PQY. Confirmed by crystal structures of the green and red forms, the photoswitching pathway involves *cis-trans* isomerization of the chromophores in both states [63].

To unravel the detailed photoactivation mechanism of IrisFP in the green state, Colletier et al. implemented time-resolved TA in 2016 [64]. They utilized a similar strategy as Yadav et al. in studying Dronpa and Dronpa-2 [44], and used fs-TA with a 400 nm pump to cover from 100 fs to 1 ns time regime and ns-TA (laser flash-photolysis) with a 410 nm pump to cover from 10 ns to 10 ms for IrisFP in pH 7 solution. Although the 400/410 nm light can also induce photoconversion, the photoactivation QY (0.5) is more than ~270-fold higher than the photoconversion QY (0.0018) [63]. Therefore, it is reasonable to consider that photoconversion contributes an extremely small portion to the observed fs-TA spectra and does not hinder the research of photoactivation of green IrisFP. Within the sub-ns window, global analysis yielded three time constants of ~100 fs, 2.02 ps, and 15.3 ps (**Figure 5**). The 100 fs component was assigned to the initial intramolecular vibrational relaxation of the chromophore, while the ~2 and 15 ps components were attributed to the lifetimes of two excited states (I_1* and I_2*) with a sequential relation, i.e., I_1* proceeds to I_2* with 2 ps time constant, then I_2* relaxes back to the original ground state and the *cis*-protonated state with 15 ps time constant (**Figure 5**). In this case, the structure of I_2* is crucial which determines the efficiency and yield of the *trans*-to-*cis* isomerization. On longer timescales (ns-ms), fitting the 490 nm absorption region yielded three exponential components in H_2O solution: 21 μs (33%), 227 μs (21%), and 2.1 ms (46% amplitude weight), all of which exhibit H/D kinetic isotope effects ranging from ~2.5 to 12, indicating that proton dissociation on these timescales may involve multiple steps or populations. This phenomenon was also observed from the TA and TRIR data of rsEGFP2 [57][60].

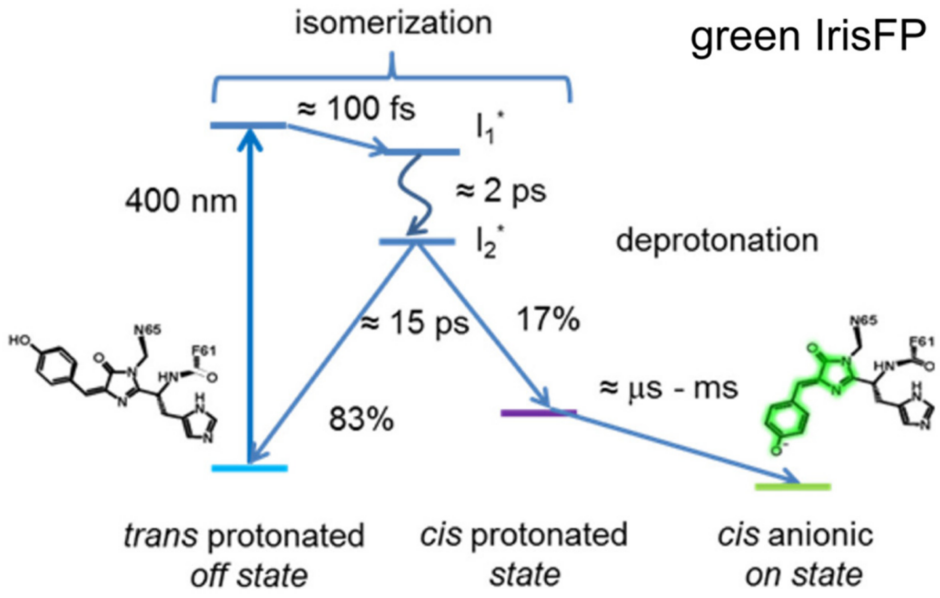

Figure 5. Photoactivation mechanism for green IrisFP in aqueous solution. Following 400 nm fs-laser excitation, the protein chromophore undergoes the excited-state *trans*-to-*cis* isomerization on the ps timescale while the deprotonation events occur on the μs-to-ms timescales. The asterisk indicates the electronic excited state for the pertinent chromophore species. Chemical structures of the chromophores in the off (dark) and on (green) states are depicted. Reprinted with permission from Ref. [64]. Copyright 2016 American Chemical Society.

Since the structures of I_1* and I_2* were unknown from the TA data, to characterize these important early-time excited-state intermediates in possible correlation with the *trans-cis* isomerization of the chromophore, the authors examined the feasibility of using SFX and an X-ray free electron laser (XFEL, 5–50 fs pulse duration) to obtain the IrisFP on-state structure. The structure was then successfully modeled based on the SFX data, also checking the mineral-grease-embedding effect on protein microcrystal structure to be minor, which closely resembles the structure retrieved from traditional (synchrotron) crystallography of a flash-cooled control crystal sample at 100 K. However, the SFX structure displays two conformers of Arg66 that can stabilize the *cis*-chromophore through H-bonds [65], and this bimodal structure may represent a more realistic case since the experiment was performed at room temperature. Notably, the authors built upon their earlier success of using SFX to solve the on-state structure of IrisFP and continued to study the photoactivation routes of rsEGFP2 in 2018 [56] and 2020 [60], wherein they reported some representative structures of intermediate states in the excited and unrelaxed ground states of a prototypical negative RSFP as summarized above.

On a related note, the researchers' lab recently implemented fs-TA and ground-state FSRS techniques to study a green-to-red photoconvertible fluorescent protein (PcFP) called the least-evolved ancestor (LEA) to retain the green phenotype with photoconversion capability [66]. Like IrisFP, this coral-derived LEA is also a tetrameric FP and can be switched between a bright and dark state in the green form with 505 nm (on-to-off) and 400 nm (off-to-on) light, respectively. Interestingly, unlike IrisFP and other RSFPs in which the photoinduced off-state species can automatically return to the bright state after dark adaptation, the light-driven off-state species in LEA is semi-trapped and cannot be turned on without light irritation [66]. This is likely due to the unique protein pocket and interactions between the LEA chromophore and local surrounding protein residues, which can undergo the photoinduced rearrangement in concert [67]. Ultrafast spectroscopic studies (fs-TA in the electronic domain, FSRS in the vibrational domain), quantum calculations, and MD simulations are ongoing in the researchers' group to characterize this intriguing semi-trapped species (still capable of photoconversion to generate red emission) that may provide the useful expanded frameworks to derive more general principles for photoswitching in competition with photoconversion.

2.4. Other Negative RSFPs

Many other negative RSFPs have been engineered from teal color to the less phototoxic redder regions, such as mTFP0.7 [41][68][69], also the monomeric rsCherryRev [70], rsTagRFP (turned on by 440 nm light and off by 567 nm light, much brighter than rsCherryRev) [71], and three rsFusionRed variants (multiple irradiation wavelengths at 405/488/510 nm can be used to switch on the protein, with 590 nm light capable of switching off the protein; faster off-switching kinetics than rsTagRFP and rsCherryRev1.4) [72], by varying the chromophore composition and mutagenesis of local residues. Note that these redder proteins (than Dronpa or rsEGFP2) display some intriguing properties from multiple switching locations [72] to an unusual planar *trans*-chromophore that is nonfluorescent [71]. However, there have not been ultrafast

studies performed on them, which represents a wonderful opportunity for researchers to implement advanced ultrafast techniques to examine these fascinating proteins. The systematic investigation and comparison of multiple negative RSFPs with contrasting properties would significantly benefit their future development in a synergistic manner. These related studies would allow the researchers to evaluate whether the retrieved ultrafast mechanisms (see above, particularly regarding the excited-state chromophore twist on the ps timescale) can be universally applied to negative RSFPs. It is expected that with a different chromophore and local protein residues, the timescales of isomerization and proton transfer would vary to different extents. However, some essential questions warrant special attention. For example, does *trans*-*cis* isomerization always occur before proton transfer? Can the researchers always see an excited-state structure that is in-between the *cis* and *trans* geometries for all RSFPs? Which local environment favors the one-bond rotation or hula twist and are these processes mutually exclusive of each other? What is the major determinant for the protonation and conformational states of the chromophore with various usual or unusual combinations of *cis*-/*trans*-/neutral/anionic/planar/nonplanar descriptors? [73] The growing pertinent comprehensive experimental findings with more advanced spectroscopic toolsets are expected to help the researchers to further understand the photoactivation mechanism from the bottom up and efficiently guide the future research directions and engineering strategies to develop next-generation negative RSFPs.

References

1. Chalfie, M.; Tu, Y.; Euskirchen, G.; Ward, W.W.; Prasher, D.C. Green fluorescent protein as a marker for gene expression. Science 1994, 263, 802–805.
2. Tsien, R.Y. The green fluorescent protein. Annu. Rev. Biochem. 1998, 67, 509–544.
3. Zimmer, M. Green fluorescent protein (GFP): Applications, structure, and related photophysical behavior. Chem. Rev. 2002, 102, 759–781.
4. Jung, G. (Ed.) Fluorescent Proteins II: Application of Fluorescent Protein Technology; Springer: Berlin/Heidelberg, Germany, 2012; p. 284.
5. Betzig, E.; Patterson, G.H.; Sougrat, R.; Lindwasser, O.W.; Olenych, S.; Bonifacino, J.S.; Davidson, M.W.; Lippincott-Schwartz, J.; Hess, H.F. Imaging intracellular fluorescent proteins at nanometer resolution. Science 2006, 313, 1642–1645.
6. Moerner, W.E. New directions in single-molecule imaging and analysis. Proc. Natl. Acad. Sci. USA 2007, 104, 12596–12602.
7. Huang, B.; Babcock, H.; Zhuang, X. Breaking the diffraction barrier: Super-resolution imaging of cells. Cell 2010, 143, 1047–1058.
8. Grotjohann, T.; Testa, I.; Leutenegger, M.; Bock, H.; Urban, N.T.; Lavoie-Cardinal, F.; Willig, K.I.; Eggeling, C.; Jakobs, S.; Hell, S.W. Diffraction-unlimited all-optical imaging and writing with a photochromic GFP. Nature 2011, 478, 204–208.
9. Chozinski, T.J.; Gagnon, L.A.; Vaughan, J.C. Twinkle, twinkle little star: Photoswitchable fluorophores for super-resolution imaging. FEBS Lett. 2014, 588, 3603–3612.
10. Shcherbakova, D.M.; Sengupta, P.; Lippincott-Schwartz, J.; Verkhusha, V.V. Photocontrollable fluorescent proteins for superresolution imaging. Annu. Rev. Biophys. 2014, 43, 303–329.
11. Bourgeois, D.; Adam, V. Reversible photoswitching in fluorescent proteins: A mechanistic view. IUBMB Life 2012, 64, 482–491.
12. Zhou, X.X.; Lin, M.Z. Photoswitchable fluorescent proteins: Ten years of colorful chemistry and exciting applications. Curr. Opin. Chem. Biol. 2013, 17, 682–690.
13. Patterson, G.H.; Lippincott-Schwartz, J. A photoactivatable GFP for selective photolabeling of proteins and cells. Science 2002, 297, 1873–1877.
14. Wachter, M.R. Photoconvertible fluorescent proteins and the role of dynamics in protein evolution. Int. J. Mol. Sci. 2017, 18, 1792.
15. Lukyanov, K.A.; Fradkov, A.F.; Gurskaya, N.G.; Matz, M.V.; Labas, Y.A.; Savitsky, A.P.; Markelov, M.L.; Zaraisky, A.G.; Zhao, X.; Fang, Y.; et al. Natural animal coloration can be determined by a nonfluorescent green fluorescent protein homolog. J. Biol. Chem. 2000, 275, 25879–25882.
16. Piatkevich, K.D.; English, B.P.; Malashkevich, V.N.; Xiao, H.; Almo, S.C.; Singer, R.H.; Verkhusha, V.V. Photoswitchable red fluorescent protein with a large Stokes shift. Chem. Biol. 2014, 21, 1402–1414.

17. Zhang, X.; Zhang, M.; Li, D.; He, W.; Peng, J.; Betzig, E.; Xu, P. Highly photostable, reversibly photoswitchable fluorescent protein with high contrast ratio for live-cell superresolution microscopy. Proc. Natl. Acad. Sci. USA 2016, 113, 10364–10369.

18. Pennacchietti, F.; Serebrovskaya, E.O.; Faro, A.R.; Shemyakina, I.I.; Bozhanova, N.G.; Kotlobay, A.A.; Gurskaya, N.G.; Bodén, A.; Dreier, J.; Chudakov, D.M.; et al. Fast reversibly photoswitching red fluorescent proteins for live-cell RESOLFT nanoscopy. Nat. Methods 2018, 15, 601–604.

19. Wazawa, T.; Noma, R.; Uto, S.; Sugiura, K.; Washio, T.; Nagai, T. A photoswitchable fluorescent protein for hours-time-lapse and sub-second-resolved super-resolution imaging. Microscopy 2021, 70, 340–352.

20. Jensen, N.A.; Jansen, I.; Kamper, M.; Jakobs, S. Reversibly switchable fluorescent proteins for RESOLFT nanoscopy. In Nanoscale Photonic Imaging; Salditt, T., Egner, A., Luke, D.R., Eds.; Springer International Publishing: Cham, Switzerland, 2020; pp. 241–261.

21. Ando, R.; Mizuno, H.; Miyawaki, A. Regulated fast nucleocytoplasmic shuttling observed by reversible protein highlighting. Science 2004, 306, 1370–1373.

22. Andresen, M.; Stiel, A.C.; Fölling, J.; Wenzel, D.; Schönle, A.; Egner, A.; Eggeling, C.; Hell, S.W.; Jakobs, S. Photoswitchable fluorescent proteins enable monochromatic multilabel imaging and dual color fluorescence nanoscopy. Nat. Biotechnol. 2008, 26, 1035–1040.

23. Brakemann, T.; Stiel, A.C.; Weber, G.; Andresen, M.; Testa, I.; Grotjohann, T.; Leutenegger, M.; Plessmann, U.; Urlaub, H.; Eggeling, C.; et al. A reversibly photoswitchable GFP-like protein with fluorescence excitation decoupled from switching. Nat. Biotechnol. 2011, 29, 942–947.

24. Arai, Y.; Takauchi, H.; Ogami, Y.; Fujiwara, S.; Nakano, M.; Matsuda, T.; Nagai, T. Spontaneously blinking fluorescent protein for simple single laser super-resolution live cell imaging. ACS Chem. Biol. 2018, 13, 1938–1943.

25. Mats Ormö; Andrew B. Cubitt; Karen Kallio; Larry A. Gross; Roger Y. Tsien; S. James Remington; Crystal Structure of the *Aequorea victoria* Green Fluorescent Protein. *Science* **1996**, *273*, 1392-1395, 10.1126/science.273.5280.1392.

26. Andresen, M.; Stiel, A.C.; Trowitzsch, S.; Weber, G.; Eggeling, C.; Wahl, M.C.; Hell, S.W.; Jakobs, S. Structural basis for reversible photoswitching in Dronpa. Proc. Natl. Acad. Sci. USA 2007, 104, 13005–13009.

27. Wilmann, P.G.; Turcic, K.; Battad, J.M.; Wilce, M.C.J.; Devenish, R.J.; Prescott, M.; Rossjohn, J. The 1.7 Å crystal structure of Dronpa: A photoswitchable green fluorescent protein. J. Mol. Biol. 2006, 364, 213–224.

28. Andre Stiel; Simon Trowitzsch; Gert Weber; Martin Andresen; Christian Eggeling; Stefan W. Hell; Stefan Jakobs; Markus Wahl; 1.8 Å bright-state structure of the reversibly switchable fluorescent protein Dronpa guides the generation of fast switching variants. *Biochemical Journal* **2007**, *402*, 35-42, 10.1042/bj20061401.

29. Mizuno, H.; Mal, T.K.; Walchli, M.; Kikuchi, A.; Fukano, T.; Ando, R.; Jeyakanthan, J.; Taka, J.; Shiro, Y.; Ikura, M.; et al. Light-dependent regulation of structural flexibility in a photochromic fluorescent protein. Proc. Natl. Acad. Sci. USA 2008, 105, 9227–9232.

30. Xin Li; Lung Wa Chung; Hideaki Mizuno; Atsushi Miyawaki; Keiji Morokuma; A Theoretical Study on the Nature of On- and Off-States of Reversibly Photoswitching Fluorescent Protein Dronpa: Absorption, Emission, Protonation, and Raman. *The Journal of Physical Chemistry B* **2009**, *114*, 1114-1126, 10.1021/jp909947c.

31. Daryna Smyrnova; Kirill Zinovjev; Iñaki Tuñón; Arnout Ceulemans; Thermal Isomerization Mechanism in Dronpa and Its Mutants. *The Journal of Physical Chemistry B* **2016**, *120*, 12820-12825, 10.1021/acs.jpcb.6b10859.

32. Yen-Cheng Chen; Amy E. Jablonski; Irina Issaeva; Daisy Bourassa; Jung-Cheng Hsiang; Christoph J. Fahrni; Robert M. Dickson; Optically Modulated Photoswitchable Fluorescent Proteins Yield Improved Biological Imaging Sensitivity. *Journal of the American Chemical Society* **2015**, *137*, 12764-12767, 10.1021/jacs.5b07871.

33. Ryoko Ando; Cristina Flors; Hideaki Mizuno; Johan Hofkens; Atsushi Miyawaki; Highlighted Generation of Fluorescence Signals Using Simultaneous Two-Color Irradiation on Dronpa Mutants. *Biophysical Journal* **2007**, *92*, L97-L99, 10.1529/biophysj.107.105882.

34. Chong Fang; Longteng Tang; Cheng Chen; Unveiling coupled electronic and vibrational motions of chromophores in condensed phases. *The Journal of Chemical Physics* **2019**, *151*, 200901, 10.1063/1.5128388.

35. Satoshi Habuchi; Ryoko Ando; Peter Dedecker; Wendy Verheijen; Hideaki Mizuno; Atsushi Miyawaki; Johan Hofkens; Reversible single-molecule photoswitching in the GFP-like fluorescent protein Dronpa. *Proceedings of the National Academy of Sciences* **2005**, *102*, 9511-9516, 10.1073/pnas.0500489102.

36. Eduard Fron; Cristina Flors; Gerd Schweitzer; Satoshi Habuchi; Hideaki Mizuno; Ryoko Ando; Frans C. De Schryver; Atsushi Miyawaki; Johan Hofkens; Ultrafast Excited-State Dynamics of the Photoswitchable Protein Dronpa. *Journal of the American Chemical Society* **2007**, *129*, 4870-4871, 10.1021/ja069365v.

37. Satoshi Habuchi; Ryoko Ando; Peter Dedecker; Wendy Verheijen; Hideaki Mizuno; Atsushi Miyawaki; Johan Hofkens; Reversible single-molecule photoswitching in the GFP-like fluorescent protein Dronpa. *Proceedings of the National Academy of Sciences* **2005**, *102*, 9511-9516, 10.1073/pnas.0500489102.

38. Mark M. Warren; Marius Kaucikas; Ann Fitzpatrick; Paul Champion; J. Timothy Sage; Jasper J. Van Thor; Ground-state proton transfer in the photoswitching reactions of the fluorescent protein Dronpa. *Nature Communications* **2013**, *4*, 1461, 10.1038/ncomms2460.

39. Andras Lukacs; Allison Haigney; Richard Brust; Kiri Addison; Michael Towrie; Gregory M. Greetham; Garth A. Jones; Atsushi Miyawaki; Peter J. Tonge; Stephen R. Meech; et al. Protein Photochromism Observed by Ultrafast Vibrational Spectroscopy. *The Journal of Physical Chemistry B* **2013**, *117*, 11954-11959, 10.1021/jp406142g.

40. Chong Fang; Renee Frontiera; Rosalie Tran; Richard A. Mathies; Mapping GFP structure evolution during proton transfer with femtosecond Raman spectroscopy. *Nature* **2009**, *462*, 200-204, 10.1038/nature08527.

41. J. Nathan Henderson; Hui-Wang Ai; Robert E. Campbell; S. James Remington; Structural basis for reversible photobleaching of a green fluorescent protein homologue. *Proceedings of the National Academy of Sciences* **2007**, *104*, 6672-6677, 10.1073/pnas.0700059104.

42. Fangyuan Han; Weimin Liu; Chong Fang; Excited-state proton transfer of photoexcited pyranine in water observed by femtosecond stimulated Raman spectroscopy. *Chemical Physics* **2013**, *422*, 204-219, 10.1016/j.chemphys.2013.03.009.

43. Ando, R.; Flors, C.; Mizuno, H.; Hofkens, J.; Miyawaki, A. Highlighted generation of fluorescence signals using simultaneous two-color irradiation on Dronpa mutants. Biophys. J. 2007, 92, L97–L99.

44. Yadav, D.; Lacombat, F.; Dozova, N.; Rappaport, F.; Plaza, P.; Espagne, A. Real-time monitoring of chromophore isomerization and deprotonation during the photoactivation of the fluorescent protein Dronpa. J. Phys. Chem. B 2015, 119, 2404–2414.

45. Kaucikas, M.; Tros, M.; van Thor, J.J. Photoisomerization and proton transfer in the forward and reverse photoswitching of the fast-switching M159T mutant of the Dronpa fluorescent protein. J. Phys. Chem. B 2015, 119, 2350–2362.

46. David W. McCamant; Philipp Kukura; Sangwoon Yoon; Richard A. Mathies; Femtosecond broadband stimulated Raman spectroscopy: Apparatus and methods. *Review of Scientific Instruments* **2004**, *75*, 4971-4980, 10.1063/1.1807566.

47. Fang, C.; Tang, L. Mapping structural dynamics of proteins with femtosecond stimulated Raman spectroscopy. Annu. Rev. Phys. Chem. 2020, 71, 239–265.

48. Nicolas Coquelle; Michel Sliwa; Joyce Woodhouse; Giorgio Schiro; Virgile Adam; Andrew Aquila; Thomas R. M. Barends; Sébastien Boutet; Martin Byrdin; Sergio Carbajo; et al. Chromophore twisting in the excited state of a photoswitchable fluorescent protein captured by time-resolved serial femtosecond crystallography. *Nature Chemistry* **2017**, *10*, 31-37, 10.1038/nchem.2853.

49. Smyrnova, D.; Zinovjev, K.; Tuñón, I.; Ceulemans, A. Thermal isomerization mechanism in Dronpa and its mutants. J. Phys. Chem. B 2016, 120, 12820–12825.

50. Samer Gozem; Hoi Ling Luk; Igor Schapiro; Massimo Olivucci; Theory and Simulation of the Ultrafast Double-Bond Isomerization of Biological Chromophores. *Chemical Reviews* **2017**, *117*, 13502-13565, 10.1021/acs.chemrev.7b00177.

51. Shimomura, O.; Johnson, F.H.; Saiga, Y. Extraction, purification and properties of Aequorin, a bioluminescent protein from the luminous Hydromedusan, Aequorea. J. Cell. Comp. Physiol. 1962, 59, 223–239.

52. Brejc, K.; Sixma, T.K.; Kitts, P.A.; Kain, S.R.; Tsien, R.Y.; Ormö, M.; Remington, S.J. Structural basis for dual excitation and photoisomerization of the Aequorea victoria green fluorescent protein. Proc. Natl. Acad. Sci. USA 1997, 94, 2306–2311.

53. Cormack, B.P.; Valdivia, R.H.; Falkow, S. FACS-optimized mutants of the green fluorescent protein (GFP). Gene 1996, 173, 33–38.

54. Grotjohann, T.; Testa, I.; Reuss, M.; Brakemann, T.; Eggeling, C.; Hell, S.W.; Jakobs, S. RsEGFP2 enables fast RESOLFT nanoscopy of living cells. eLife 2012, 1, e00248.

55. Mariam El Khatib; Alexandre Martins; Dominique Bourgeois; Jacques-Philippe Colletier; Virgile Adam; Rational design of ultrastable and reversibly photoswitchable fluorescent proteins for super-resolution imaging of the bacterial periplasm. *Scientific Reports* **2016**, *6*, srep18459, 10.1038/srep18459.

56. Coquelle, N.; Sliwa, M.; Woodhouse, J.; Schirò, G.; Adam, V.; Aquila, A.; Barends, T.R.M.; Boutet, S.; Byrdin, M.; Carbajo, S.; et al. Chromophore twisting in the excited state of a photoswitchable fluorescent protein captured by time-resolved serial femtosecond crystallography. Nat. Chem. 2018, 10, 31–37.

57. Uriarte, L.M.; Vitale, R.; Niziński, S.; Hadjidemetriou, K.; Zala, N.; Lukacs, A.; Greetham, G.M.; Sazanovich, I.V.; Weik, M.; Ruckebusch, C.; et al. Structural information about the trans-to-cis isomerization mechanism of the photoswitchable fluorescent protein rsEGFP2 revealed by multiscale infrared transient absorption. J. Phys. Chem. Lett. 2022, 13, 1194–1202.

58. Jeffrey Chang; Matthew G. Romei; Steven G. Boxer; Structural Evidence of Photoisomerization Pathways in Fluorescent Proteins. *Journal of the American Chemical Society* **2019**, *141*, 15504-15508, 10.1021/jacs.9b08356.

59. Virgile Adam; Kyprianos Hadjidemetriou; Nickels Jensen; Robert L. Shoeman; Joyce Woodhouse; Andrew Aquila; Anne-Sophie Banneville; Thomas R. M. Barends; Victor Bezchastnov; Sébastien Boutet; et al. Rational control of structural off-state heterogeneity in a photoswitchable fluorescent protein provides switching contrast enhancement. *bioRxiv* **2021**, *New_Results*, DOI: https://doi.org/10.1101/2021.11.05.462999, 10.1101/2021.11.05.462999.

60. Woodhouse, J.; Nass Kovacs, G.; Coquelle, N.; Uriarte, L.M.; Adam, V.; Barends, T.R.M.; Byrdin, M.; de la Mora, E.; Bruce Doak, R.; Feliks, M.; et al. Photoswitching mechanism of a fluorescent protein revealed by time-resolved crystallography and transient absorption spectroscopy. Nat. Commun. 2020, 11, 741.

61. Laptenok, S.P.; Gil, A.A.; Hall, C.R.; Lukacs, A.; Iuliano, J.N.; Jones, G.A.; Greetham, G.M.; Donaldson, P.; Miyawaki, A.; Tonge, P.J.; et al. Infrared spectroscopy reveals multi-step multi-timescale photoactivation in the photoconvertible protein archetype Dronpa. Nat. Chem. 2018, 10, 845–852.

62. Jörg Wiedenmann; Sergey Ivanchenko; Franz Oswald; Florian Schmitt; Carlheinz Röcker; Anya Salih; Klaus-Dieter Spindler; G. Ulrich Nienhaus; EosFP, a fluorescent marker protein with UV-inducible green-to-red fluorescence conversion. *Proceedings of the National Academy of Sciences* **2004**, *101*, 15905-15910, 10.1073/pnas.0403668101.

63. Adam, V.; Lelimousin, M.; Boehme, S.; Desfonds, G.; Nienhaus, K.; Field, M.J.; Wiedenmann, J.; McSweeney, S.; Nienhaus, G.U.; Bourgeois, D. Structural characterization of IrisFP, an optical highlighter undergoing multiple photo-induced transformations. Proc. Natl. Acad. Sci. USA 2008, 105, 18343–18348.

64. Jacques-Philippe Colletier; Michel Sliwa; François-Xavier Gallat; Michihiro Sugahara; Virginia Guillon; Giorgio Schirò; Nicolas Coquelle; Joyce Woodhouse; Laure Roux; Guillaume Gotthard; et al. Serial Femtosecond Crystallography and Ultrafast Absorption Spectroscopy of the Photoswitchable Fluorescent Protein IrisFP. *The Journal of Physical Chemistry Letters* **2016**, *7*, 882-887, 10.1021/acs.jpclett.5b02789.

65. Colletier, J.-P.; Sliwa, M.; Gallat, F.-X.; Sugahara, M.; Guillon, V.; Schirò, G.; Coquelle, N.; Woodhouse, J.; Roux, L.; Gotthard, G.; et al. Serial femtosecond crystallography and ultrafast absorption spectroscopy of the photoswitchable fluorescent protein IrisFP. J. Phys. Chem. Lett. 2016, 7, 882–887.

66. Krueger, T.D.; Tang, L.; Zhu, L.; Breen, I.L.; Wachter, R.M.; Fang, C. Dual illumination enhances transformation of an engineered green-to-red photoconvertible fluorescent protein. Angew. Chem. Int. Ed. 2020, 59, 1644–1652.

67. Kim, H.; Zou, T.; Modi, C.; Dörner, K.; Grunkemeyer, T.J.; Chen, L.; Fromme, R.; Matz, M.V.; Ozkan, S.B.; Wachter, R.M. A hinge migration mechanism unlocks the evolution of green-to-red photoconversion in GFP-like proteins. Structure 2015, 23, 34–43.

68. Hui-Wang Ai; J. Nathan Henderson; S. James Remington; Robert E. Campbell; Directed evolution of a monomeric, bright and photostable version of *Clavularia* cyan fluorescent protein: structural characterization and applications in fluorescence imaging. *Biochemical Journal* **2006**, *400*, 531-540, 10.1042/bj20060874.

69. Hui-Wang Ai; Robert E. Campbell; Teal fluorescent proteins: characterization of a reversibly photoswitchable variant. *Biomedical Optics (BiOS) 2008* **2008**, *6868*, 68680D-68680D-7, 10.1117/12.761423.

70. Andre C. Stiel; Martin Andresen; Hannes Bock; Michael Hilbert; Jessica Schilde; Andreas Schönle; Christian Eggeling; Alexander Egner; Stefan W. Hell; Stefan Jakobs; et al. Generation of Monomeric Reversibly Switchable Red Fluorescent Proteins for Far-Field Fluorescence Nanoscopy. *Biophysical Journal* **2008**, *95*, 2989-2997, 10.1529/biophysj.108.130146.

71. Sergei Pletnev; Fedor V. Subach; Zbigniew Dauter; Alexander Wlodawer; Vladislav V. Verkhusha; A Structural Basis for Reversible Photoswitching of Absorbance Spectra in Red Fluorescent Protein rsTagRFP. *Journal of Molecular Biology* **2012**, *417*, 144-151, 10.1016/j.jmb.2012.01.044.

72. Francesca Pennacchietti; Ekaterina O. Serebrovskaya; Aline R. Faro; Irina I. Shemyakina; Nina G. Bozhanova; Alexey A. Kotlobay; Nadya G. Gurskaya; Andreas Bodén; Jes Dreier; Dmitry M. Chudakov; et al. Fast reversibly photoswitching red fluorescent proteins for live-cell RESOLFT nanoscopy. *Nature Methods* **2018**, *15*, 601-604, 10.1038/s41592-018-0052-9.

73. Longteng Tang; Chong Fang; Fluorescence Modulation by Ultrafast Chromophore Twisting Events: Developing a Powerful Toolset for Fluorescent-Protein-Based Imaging. *The Journal of Physical Chemistry B* **2021**, *125*, 13610-13623, 10.1021/acs.jpcb.1c08570.